Seismogenic fault characterization in the Pollino area (Southern Italy)

F. Napolitano(1) on behalf of A. Gervasi(2)(3), M. La Rocca(3), D. Galluzzo(2), I. Guerra(3) and R. Scarpa(1)

(1) *Università degli Studi di Salerno - Via Giovanni Paolo II, 84084, Fisciano (SA), Italy*
(2) *Istituto Nazionale di Geofisica e Vulcanologia - Via di Vigna Murata, 605, 00143 Roma, Italy*
(3) *Università della Calabria - Ponte P. Bucci, 87036, Rende (CS), Italy*

Summary. — One of the most intense periods of the 2010–2014 Pollino swarm (Southern Italy), namely from November 2011 to April 2012, has been analyzed with the aim of a precise relocation of the hypocenters in order to image the seismogenetic structure(s) responsible for this swarm. Using recordings of temporary and permanent stations installed in the area during the sequence, we identified 18 clusters of earthquakes characterized by extremely similar waveforms, selected through a cross-correlation analysis. We performed a relative location of each event of each cluster. For each cluster the spatial distribution of hypocenters was fitted by a plane to infer the fault plane orientation. We compared the results with the focal mechanism of individual earthquakes of the same cluster. For an overall view of the relative position of each reference event of all analyzed clusters, we performed the relative location of all these master events adjusted to take into account the different shapes of the waveforms. The results show that different clusters are likely patches of the same fault plane, mostly parallel among them and with similar focal mechanisms, with a strike angle in the NW-SE direction and dip around 35–45 degrees, deepening SW toward the Tyrrhenian sea. The absolute location gives a depth distribution between 4.5 and 6 km b.s.l.

1. – Introduction

Small magnitude earthquakes offer the best way to image crustal fault structures, especially when they occur in swarms that last for long periods of time in a localized area. This opportunity is particularly useful in areas where large earthquakes have not been observed during the last centuries. Despite the low signal-to-noise ratio typical of small magnitude events, the advantage of using such small earthquakes is that, according
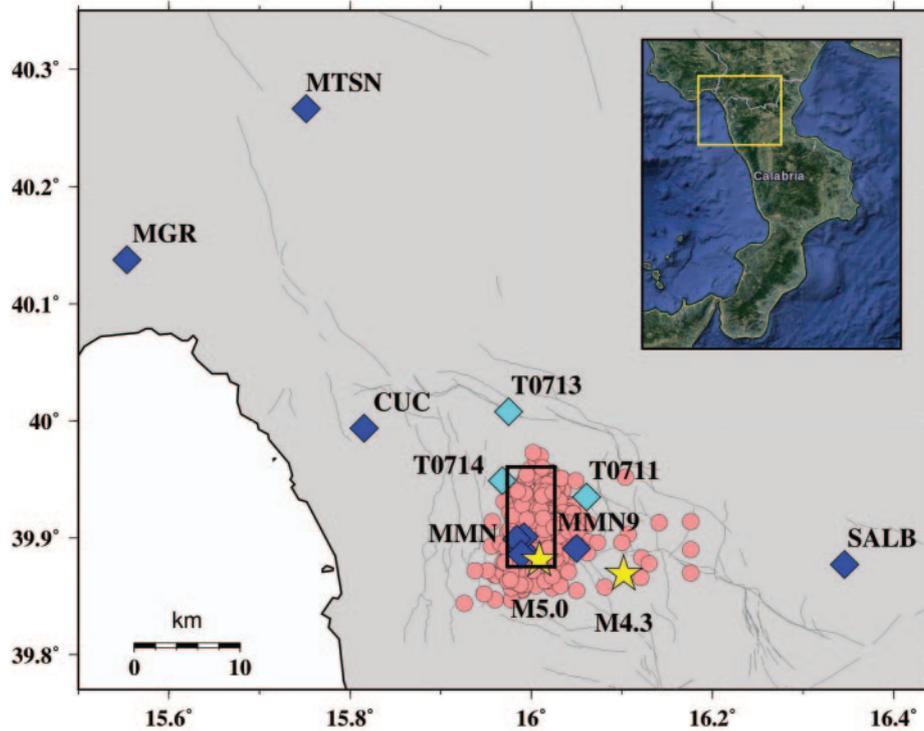
Fig. 1. – Map of the Pollino area: pink circles represent the hypocenters of the sequence between November 2011 and April 2012, blue and cyan diamonds represent the permanent and temporary stations stations used in this work, respectively. The yellow stars represent the two main shocks of the 2010–2014 Pollino sequence. Faults in the background are taken from the work of [7]. The rectangle in the center of the sequence represents the areas highlighted in fig. 4.

to the Gutenberg and Richter law, they provide a large amount of data useful for imaging fault structures.

Relative locations of earthquakes is a consolidated approach in seismology. This methodology is crucial to reduce the uncertainty associated with absolute locations, typically due to human error in picking P- and S-waves, inadequate seismic stations coverage, unreliable velocity model, and so on [1]. Reducing the error using relative locations of earthquakes of similar waveforms with respect to one *master event* is crucial to obtain a more realistic imaging of seismic structures.

Relative location techniques are mostly applied to sequences of events occurring very close to each other compared to the source-receiver distance, characterized by similar waveform and magnitude. For this reason, we aim to apply this methodology to one of the largest swarm of the last decades: the 2010–2014 Pollino sequence.

The Pollino area, located in Southern Italy between Calabria and Basilicata (fig. 1), was affected between 2010 and 2014 by a swarm-like sequence of more than 6000 earthquakes of $M > 1$. The events of the sequence were located in two contiguous but separated areas, the so-called *eastern* and *western* clusters. In fig. 1 we only show the western cluster, the area where all the seismicity analyzed in this paper took place. These events were characterized by shallow depth (0–10 km), spatial distribution of less than

30×15 km and by low or moderate magnitude. Two were the main-shocks of the sequence (yellow stars in fig. 1): the $M_L 4.3$ on 28 May 2012 and the $M_L 5.0$ on 26 October 2012 [2-5]. Several temporary stations were installed in the surrounding area [6] to better monitor the evolution of the swarm and to improve the locations of the hypocenters. Some of these stations became permanent (blue diamonds in fig. 1, while others were removed or relocate to other sites during the sequence (cyan diamonds in fig. 1). The same seismic traces have also been used in recent works in combination with geological and remote-sensing data to map seismically-active faults [7] and to evaluate local site effects [8] in the area.

In this work we aim to use the high-quality waveforms recorded by this seismic network to perform the relative locations of the hypocenters, grouped in clusters of similar waveforms, using a methodology developed by [1] based on the computation of time differences between the current event and the master event at each station. Moreover, in order to image with extreme accuracy the fault structures responsible for the 2010–2014 Pollino swarm and to assess their source mechanisms, we also compute: the best fit plane of the hypocenters of each cluster; the focal mechanisms of the master events of each cluster, chosen considering the highest signal-to-noise ratio at larger epicentral distance and the best azimuthal coverage of seismic stations; the synthetic seismograms to be compared with the waveforms recorded at different stations to confirm the computed focal mechanisms; the rupture length of each patch of the main fault to be compared with the spatial distribution of the hypocenters resulting from the relative location procedure.

2. – Data and methodology

The dataset used in this work consists of velocity waveforms recorded between November 2011 and April 2012, one of the most intense activity periods of the swarm [4,6].

During the selected time period the sequence developed mainly in the western sector (pink circles in fig. 1). None of the two main shocks that characterized the sequence occurred in this time range. The seismic network, installed and operated by *Università della Calabria* and *Istituto Nazionale di Geofisica e Vulcanologia (INGV)*, changed many times following the evolution of the swarm. The number of stations increased during the period of our analysis, reaching a total number of permanent and temporary stations of 12 within an epicentral distance of 50 km. The number of available seismic stations was the most important reason we chose this time period. An automatic P-wave picking was applied to the continuous recordings at the reference station, MMN. After a visual inspection of the automatically picked waveforms, we obtained a catalog of 3263 earthquakes to work on.

The following step was the application of the cross-correlation analysis in order to select earthquake pairs characterized by very similar waveforms, which means they likely occurred on the same fault and with very similar focal mechanisms. We computed the normalized cross-correlation on band-pass filtered signals between 3 and 15 Hz, over a 3 seconds time window starting 0.5 seconds before the P-wave onset. We selected all event pairs characterized by cross-correlation greater than 0.85 and amplitude greater than 1500 counts, at the station MMN, which roughly corresponds to magnitude $M_L = 0.6$, excluding those earthquakes whose signal-to-noise ratio is too low to give reliable results. The selection based on the cross-correlation analysis gave as output 294 earthquakes grouped in 18 clusters of events with similar waveforms (an example of waveforms in a cluster is shown in fig. 2 at the station MMN for the cluster 205) composed by a number
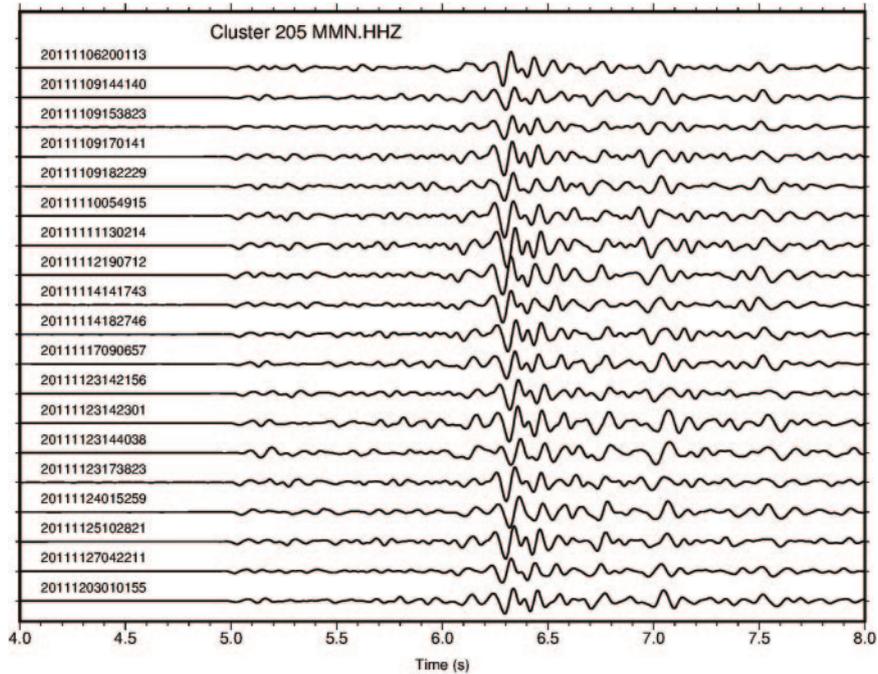
Fig. 2. – Example of a cluster of similar waveforms. We show 19 of the 32 waveforms, recorded at station MMN, for the cluster 205, the largest among all the clusters extracted through the cross-correlation analysis.

of waveforms that varies from a minimum of 9 to a maximum of 32 earthquakes per cluster.

The changing number of events for the different clusters and the low percentage of clusterized events with respect to the 3263 starting events can be explained pointing out the limits of the dataset. The small size of the fault patches that generate each cluster (we require at least 5 events to perform a reliable analysis), and the low SNR of smaller events at the furthest stations are a limitation directly related to the source. Adding problems related to the seismic stations, such as the small number and/or inappropriate azimuthal coverage of the stations around the epicenter, the occurrence of other similar earthquakes in periods not analyzed because of an inadequate number of stations, and the loss of waveforms due to technical problems at some stations (that plays a crucial role when the number of stations is barely sufficient for an ideal analysis) the reasons of the loss of a large quantity of information become clear.

2˙1. *Relative locations*. – For each of the 18 clusters we chose a reference event, the so-called *master event* characterized by the highest signal-to-noise ratio among all the earthquakes of the cluster and by the best azimuthal coverage of the seismic stations. We perform the absolute locations of these master events using the velocity model given by [9]. We applied a simple method of relative location, developed by [1] based on the computation of time differences between the current event and the master event at each station. This method is effective if the distance between the two hypocenters is much smaller compared with the source-receiver distance. At this scale the velocity around

the hypocentral position is assumed constant, so the cause of a relative time difference between nearly identical ray paths has to be the slightly different spatial location of the hypocenters.

We name the relative hypocenter coordinates $(\Delta x, \Delta y, \Delta z, \Delta T_0)$ of an event related to the master event. Naming ϕ and θ the azimuth and take-off angles at the k-th seismic station, time delays Δt_N, computed on signals resampled at 500 sps are used to compute the hypocenters coordinate differences $(\Delta x, \Delta y, \Delta z, \Delta T_0)$ through the solution of the following matrix equation:

$$\frac{1}{v} \begin{pmatrix} \sin\theta_1 \sin\phi_1 & \sin\theta_1 \cos\phi_1 & -\cos\theta_1 & v \\ \sin\theta_2 \sin\phi_2 & \sin\theta_2 \cos\phi_2 & -\cos\theta_2 & v \\ \vdots & \vdots & \vdots & \vdots \\ \sin\theta_N \sin\phi_N & \sin\theta_N \cos\phi_N & -\cos\theta_N & v \end{pmatrix} \begin{pmatrix} \Delta x \\ \Delta y \\ \Delta z \\ \Delta T_0 \end{pmatrix} = \begin{pmatrix} \Delta t_1 \\ \Delta t_2 \\ \vdots \\ \Delta t_N \end{pmatrix},$$

which is an overdetermined system, whose solution is given by

$$(1) \qquad\qquad m = (G^T G)^{-1} G^T d,$$

which represent the relative locations of each event compared to the master event.

Using a MATLAB routine we:

- band-pass filter the waveforms;

- assess the travel time difference from the cross-correlation;

- invert the matrix previously shown, achieving the relative positions of the hypocenters with respect to the master event.

Note: in the MATLAB routine, azimuth and take-off angles are taken from the absolute location of the master event. To assess the stability and reliability of the analysis we use different corner frequencies, windows of analysis and phases:

- corner frequencies: 2–12 Hz and 2–15 Hz;

- window lengths: 2 s and 3 s;

- phases: P and S waves.

For both P and S waves, the starting point of the window of analysis is 0.5 seconds before the onset of the used phase.

2˙2. *Hypocenters fitting plane.* – All the hypocenters of each cluster were plotted in a 3D image and fitted by a plane, $f(x,y) = ax + by + c$, computed to find the orientation of the fault that likely produced those earthquakes (fig. 3), evaluating the strike and the dip angle, λ and δ respectively, from the equations

$$(2) \qquad\qquad \lambda = \text{atan}(-b/a) \quad \delta = \text{atan}(\sqrt{a^2 + b^2}).$$

We computed these angles just to have a benchmark for the following analysis in order to confirm the reliability of the methodology. It is clear that the hypocenter distribution, and consequently the best fitting plane, should be more realistic depending on the number of earthquakes and on the azimuthal coverage of the stations around the source.
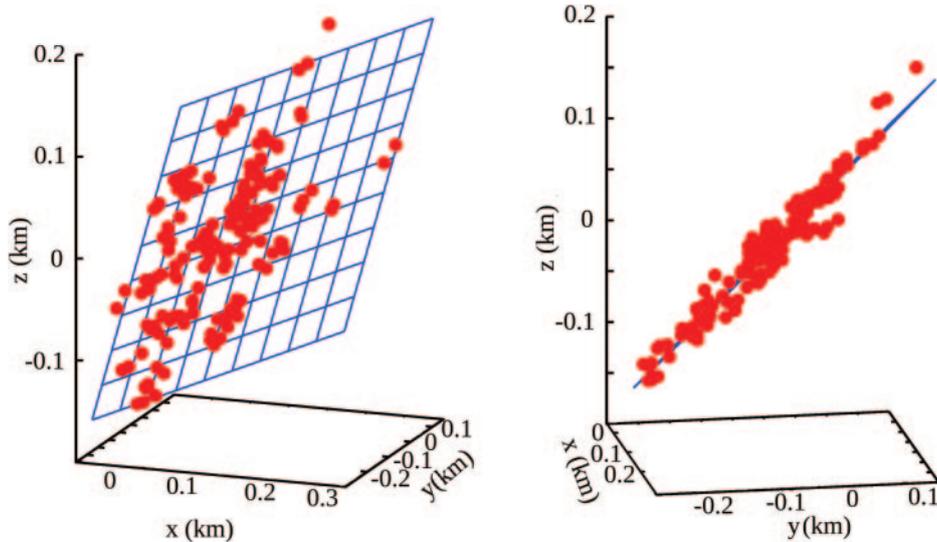
Fig. 3. – Example of relative location of the cluster 205. Red circles are the hypocenters relocated through eq. (1), while the blue plane represents the best fitting plane computed for this cluster.

2˙3. *Magnitude assessment and rupture size.* – Often during a swarm some earthquakes, not necessarily the smallest ones, can be missed by automatic procedures. This can happen for example if two or more earthquakes occur within few seconds. Our analysis could include these missed earthquakes as a part of the cluster. Therefore beside their absolute and relative location, we computed also their magnitude through a relationship based on the signal duration. For many earthquakes present in the catalog we compared their *local magnitude* with the *duration magnitude*. From the last square fitting of the two magnitudes we got the best parameters for the duration magnitude, obtaining the following relationship:

$$(3) \qquad\qquad M_d = 2.2 \log(d) - 1.4,$$

where d is the earthquake duration estimated from the logarithm of RMS of band-pass filtered signals (1 Hz–20 Hz) averaged among the three components, and assuming the event ends when the S-coda amplitude returns to the same seismic noise level as before the event [10]. This method is useful because the duration magnitude is a reliable and fast method to assess magnitude expecially for small and very small earthquakes.

We estimated the earthquake source size from the corner frequency of displacement spectra corrected for the attenuation. The rupture time corresponding to the corner frequency was used to compute the rupture length assuming $V_s = 3$ km/s at the source and $V_r = 0.9 V_s$:

$$(4) \qquad\qquad l_{rupt} = \frac{v_r}{f_c},$$

where f_c is the corner frequency and v_r the rupture velocity.

For each cluster the source size of individual events was compared with the size of relative hypocenter distribution.
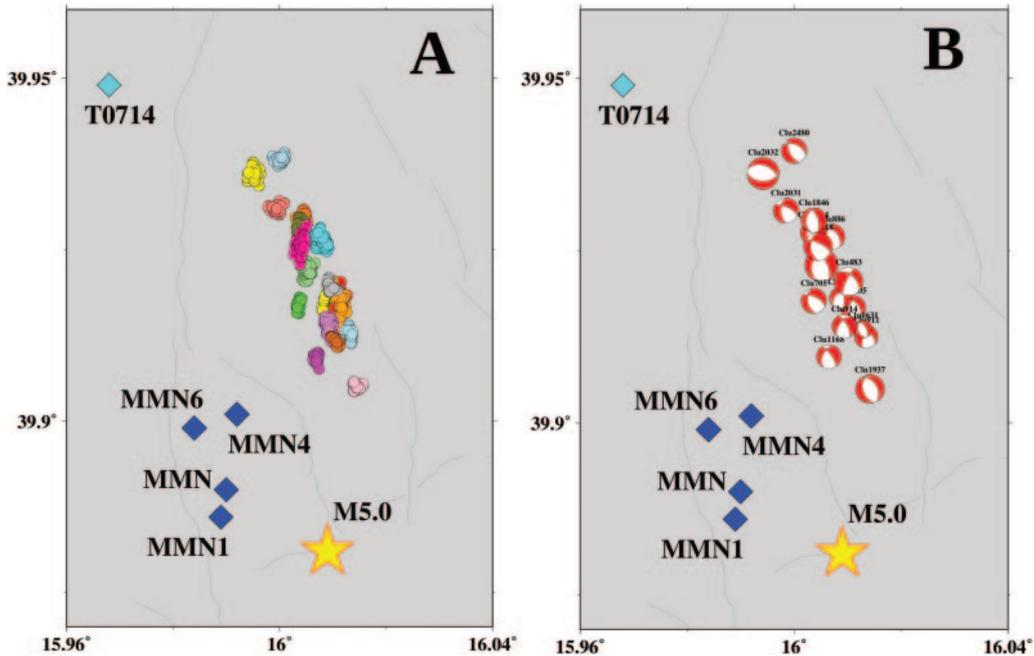
Fig. 4. – Area of the map contained in the black rectangle drawn in fig. 1. Panel A shows the 18 clusters analyzed in the period November 2011–April 2012 with different colours, while Panel B shows the focal mechanisms computed for each master event of the clusters. Blue and cyan diamonds represent the closest permanent and temporary stations, the yellow star represents the main-shock of $M5.0$.

2˙4. *Focal mechanisms and synthetic seismogram assessment*. – Crucial for our purpose is the focal mechanisms evaluation for each master event. In the Pollino area several focal mechanisms were evaluated [3] for magnitude greater than $M_L2.7$. We further reduced this threshold, reaching $M_L1.2$ as the lowest threshold of magnitude (fig. 4).

We computed the focal mechanisms using the program FOCMEC [11] that uses the polarity of the first arrival P and S. In some cases the waveform similarity has been used to improve the signal to noise ratio through the signal stacking, thus improving the SNR and helping the reading of P and S wave polarity in case of small events at the farthest stations. We therefore used these mechanisms as input, together with azimuth, take-off angle and epicentral distance to compare the synthetic seismogram achieved using these mechanisms with the real seismograms. In this way we could have another validation of the results achieved by the relocation method. Synthetic seismograms were computed using the indications contained in *Computer programs in seismology* [12].

2˙5. *Relative location of all clusters*. – After the relative location of each cluster, we wanted to compare the location of any clusters with the others, therefore we performed the relative location of the 18 master events with respect to that recorded by the highest number of stations (cluster 1262). Since the master events do not have waveforms as similar as the individual cluster events, we applied the following slightly different process. The waveforms, oversampled at 500 sps, were bandpass filtered between 10 Hz and 20 Hz, then the signals were manually cut by retaining only the first 3 pulses after a

short window of noise. Finally, we multiplied by -1 all signals whose P-wave first pulse was negative. After this procedure all signals show the earthquake starting by a positive pulse, and are very similar due to the high frequency band. The cross-correlation of these signals gives an estimate of the time differences to be used for the relative location with the same method applied for any clusters. An accurate preparation of the waveforms is crucial to obtain a reliable location of the master events among them. Filtering and waveform inversion is an important step to make waveforms produced by faults characterized by different focal mechanisms or quite distant from each other, similar enough to estimate the time differences.

2˙6. *Absolute locations of all events*. – Giving a look at the Italian Seismological Instrumental Database (ISIDe), ISIDe Working Group, 2016, we found some discrepancy between the locations of events contained in the same cluster, so related by an high cross-correlation value. To improve our analysis we performed also the absolute locations of the 294 events on which we had performed the relative locations, using both HYPOSAT [13] and a self-made software.

3. – Results and discussion

The main aim of this work is a detailed imaging of the faults responsible for the 2010–2014 seismic swarm in the Pollino area (Southern Italy) for a better knowledge of the spatial and temporal behavior of the seismicity and to relate it with the previous geological and statistical studies in the area [3, 4, 7].

We applied relative locations of selected clusters of earthquakes of similar waveforms during the swarm in order to reduce as much as possible the uncertainty due to the velocity model and to make the resulting structure dependent only on the accurate absolute location of a single event, characterized by an high signal-to-noise ratio and by the best azimuthal coverage. Due to the lack of a sufficient number of seismic stations in various periods during the swarm, we chose the period November 2011–April 2012 when the area was well-covered on average by no less than 8 seismic stations. We grouped earthquakes characterized by similar waveforms (cross-correlation threshold of 0.85) in clusters, changing parameters during each location to test the reliability of the results (excluding the events moving away from the cluster changing these parameters), performing the best fit plane, evaluating the magnitude, focal mechanism and rupture length of each plane. The fault patches of the main fault, highlighted by the best fitting plane of each cluster, have a rupture length in the range between 150 and 400 meters, with a nearly circular shape as expected for small rupture zones. The entire fault plane (fig. 5), obtained from the joining of all the clusters relocated with the procedure explained in sect. 2˙5, is characterized by an area of $2 \times 3\,\mathrm{km}^2$, located $4.4\,\mathrm{km}$ from Mormanno (Cosenza) in the north-east direction, at a depth between 4.5 and 6 km b.s.l. The focal mechanisms evaluated for each cluster and the following comparison with the synthetic seismograms at each station confirm the orientation of the fault plane. Looking at the clusters and their mechanisms individually we achieve: strike ranging between $110°$ and $170°$, dip between $35°$ and $45°$ and rake ranging from $-50°$ to $-150°$. The last information suggests a mechanism of *normal fault*, with a strong lateral component in some cases different between a cluster and another. These results fit with the several number of focal mechanisms computed by [3] and confirmed by [4], for events at that depth indicating normal source mechanisms. These results are also in agreement with the extensional stress regime of the region [7, 14].
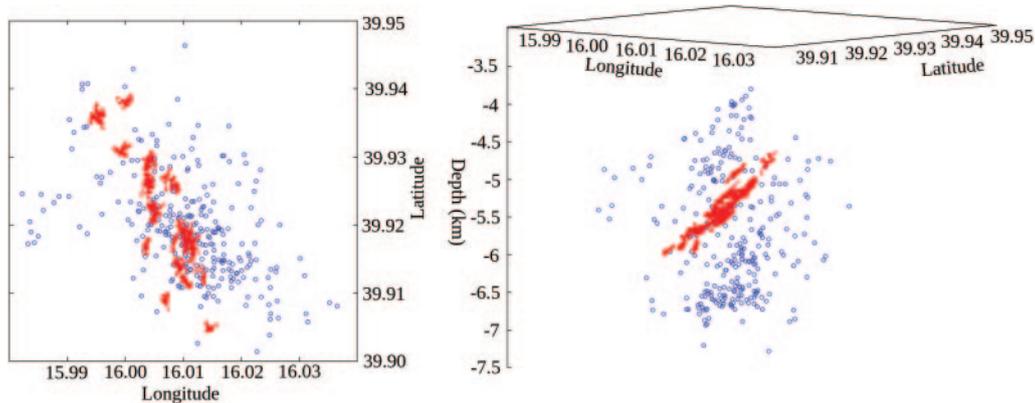
Fig. 5. – Results obtained performing the relative location of all the clusters. Blue circles represent the absolute location of the 294 events computed in this work. Red circles represent the relative locations of all the clusters, drawing a well defined fault structure, responsible for the clustered events of the sequence between November 2011 and April 2012.

4. – Conclusions

This work shows the analysis of one of the most intense periods of activity during the 2010–2014 Pollino seismic swarm, namely between November 2011 and April 2012. Seismic waveforms have been used to relocate earthquakes in order to image the fault(s) responsible for that part of the swarm. Results of relative location show a single normal fault oriented NW-SE, dipping SW toward the Tyrrhenian sea with a dip angle around 40°. Hundreds of small earthquakes occurred on small patches of this fault, each one producing earthquakes characterized by very similar waveforms. On the other hand, most of the earthquakes which occurred in the period of analysis show different waveforms and are located in a volume much larger than the identified fault. That indicates a highly fractured volume of the crust beneath Mt. Pollino where strain energy is released through thousands of small earthquakes not all generated by the same fault. Further data related to the second most intense period of the swarm will be analyzed to achieve other results for a complete knowledge of all the features of the fault responsible for the swarm.

REFERENCES

[1] Got J.-L. *et al.*, *J. Geophys. Res.*, **99** (1994) 15375.
[2] Totaro C. *et al.*, *Seismol. Res. Lett.*, **84** (2013) 955.
[3] Totaro C. *et al.*, *B. Seismol. Soc. A.*, **105** (2015) 3121.
[4] Passarelli L. *et al.*, *Geophys. J. Int.*, **201** (2015) 1553.
[5] Cheloni D. *et al.*, *Sci. Rep UK*, **7** (2017) 1.
[6] Margheriti L. *et al.*, Rapporti Tecnici INGV, 252 (2013).
[7] Brozzetti F. *et al.*, *J. Struct. Geol.*, **94** (2017) 13.
[8] Napolitano F. *et al.*, *B. Seismol. Soc. Am.*, **108** (2018) 309.
[9] Barberi G. *et al.*, *Phys. Earth Planet. Inter.*, **147** (2004) 297.

[10] SATO H. and FEHLER M. C., *Seismic Wave Propagation and Scattering in the Heterogeneous Earth* (Springer-Verlag, New York) 1998.

[11] SNOKE J. A., *Earthquake mechanisms*, in *Encyclopedia of Geophysics*, edited by JAMES D. E. (Van Nostrand Reinhold Company, New York) 1989, pp. 239–245.

[12] HERRMANN R. B., *Seismol. Res. Lett.*, **84** (2013) 1081.

[13] SCHWEITZER J., *Pure Appl. Geophys.*, **158** (2001) 277.

[14] FERRANTI L. *et al.*, *Tectonophysics*, **721** (2017) 372.